UNIVERSITY OF COPENHAGEN

# Reduced early life mucosal integrity decreases thymic cell counts and increases local, but not thymic regulatory, T cell recruitment: Gut mucosal integrity breach and thymic T cells

Zakariassen, Hannah Louise; Bendtsen, Katja Maria; Tougaard, Peter; Hansen, Axel Kornerup

*Original Research Article*

# Reduced early life mucosal integrity decreases thymic cell counts and increases local, but not thymic regulatory, T cell recruitment: Gut mucosal integrity breach and thymic T cells

Hannah Louise Zakariassen, (iD) Katja Maria Bendtsen,
Peter Tougaard and Axel Kornerup Hansen

## Abstract

Early life immune gut microbiota contact is critical for regulatory T cell–mediated oral tolerance induction. We induced a mucosal integrity breach with low dextran sulfate sodium dose right after weaning in BALB/c mice along with a standard high dose to study the impact of increased gut microbiota lymphatic tissue contact on the thymus. Both doses increased gut permeability, which caused a short-term generalized thymic involution and regulatory T cell induction in the mesenteric lymph nodes, even in the absence of clinically apparent inflammation in the low-dose group. The thymic regulatory T cells resisted thymic involution. In the low-dose group, we found acutely altered gut mobilization patterns characterized by changed gut-homing marker CD103 expression on mesenteric lymph node $CD4^+$ T cells as well as on mature $CD8^+$ T cells and developing $CD4^-/CD8^-$ thymocytes. Furthermore, CD218a (IL-18-receptor-a) expression was acutely decreased on both mature $CD8^+$ T cells and regulatory T cells, while increased on the mesenteric lymph node $CD8^+$ T cells, indicating a direct link between the thymus and the mesenteric lymph nodes with CD218a in a functional role in thymic involution. Acute and non-persisting regulatory responses in the mesenteric lymph nodes were induced in the form of a relative regulatory T cell increase. We saw no changes in total thymic regulatory T cells and thus the thymus does not seem to play a major role of in the regulatory immunity induced by increased gut microbiota lymphatic tissue contact around weaning, which in our study primarily was located to the gut.

## Keywords

cytotoxic T cells, gut microbiota, helper T cells, regulatory T cells, thymocytes

Date received: 5 September 2018; accepted: 12 December 2018

## Introduction

Insufficient microbial exposure during early age, for example, because human gut microbiota (GM) diversity is decreasing,[1] may be hypothesized to induce predisposition for allergic, inflammatory, and autoimmune diseases[2] due insufficient induction of oral tolerance.[3] Forkhead box p3 ($Foxp3^+$) $CD25^+$ regulatory T cells (Tregs) play an important

Section of Experimental Animal Models, Department of Veterinary and Animal Sciences, Faculty of Health and Medical Sciences, University of Copenhagen, Frederiksberg C, Denmark

**Corresponding author:**
Hannah Louise Zakariassen, Section of Experimental Animal Models, Department of Veterinary and Animal Sciences, Faculty of Health and Medical Sciences, University of Copenhagen, Thorvaldsensvej 57, DK-1871 Frederiksberg C, Denmark.
Email: hlza@sund.ku.dk

role in the suppression of gut mucosa auto-reactivity,[4–9] and interleukin (IL)-10 is a key immune-modulatory factor.[10,11] Rodent studies point out a window of possible immunomodulation in either the post-partum[12–14] or the post-weaning period.[15] Antibiotic treatment in neonatal mice increases atopic disease severity,[16] and germ-free (GF) conditions during the first weeks of life lead to maturation defects of gut-associated lymphoid tissues (GALTs) and the spleen and dysfunctional natural killer T cell (NKT) function.[12,13] Furthermore, post-weaning GM inoculation in GF mice permanently alters immune functions.[15]

The mucin-feeding bacterium *Akkermansia muciniphila* with an abundance of up to 3% of the gut bacteria[17] is protective against, for example, type 1 diabetes (T1D),[18,19] inflammatory bowel disease (IBD),[20] autism,[21] and diet-induced obesity.[22] Previously, we developed a mouse model, in which a low dose of drinking water dextran sulfate sodium (DSS) is used as an artificial mucin degrader,[23] which increased the abundance of *A. muciniphila* and decreased the abundance of segmented filamentous bacteria (SFBs).[23] We also observed increased Tregs in the mesenteric lymph nodes (MLNs) and the spleen, and decreased natural killer (NK) and NKT cells, while colonic expression of Foxp3 and Il1a was twofold upregulated 25 days after treatment.[23] Vancomycin lowers the incidence of T1D in newborn T1D-prone non-obese diabetic (NOD) mice, and it propagates both *A. muciniphila* and proteobacteria-carrying lipopolysaccharide (LPS), which is a microbial-associated molecular pattern (MAMP).[19] LPS induces NFκB-mediated inflammation through Toll-like receptor 4.[24] This increased MAMP-GALT contact in early life may have a long-term protective role. Early life low-dose DSS treatment of NOD mice does not reduce the incidence of the T helper cell (Th) type 1 dominated T1D,[25] while it significantly reduces later life local acute tissue inflammation in the Th type 2 dominated oxazolone IBD model.[26] Therefore, further elucidation of early life MAMP-GALT contact is needed. Previous studies on early life induction of regulatory immunity have focused on either the gut or the systemics, but also the thymus may have a role. Thymic development of lymphoid progenitor cells through double negative CD4$^-$CD8$^-$ (DN), double positive CD4$^+$ CD8$^+$ (DP), and single positive CD4$^+$CD8$^-$/CD4$^-$CD8$^+$ (SP) thymocyte stages followed by positive and negative selection secures

continuous release to the periphery of naïve effector T cells with central tolerance.[27] Contrary to conventional thymic selection, thymus-developed Tregs (tTregs) pass through agonist selection thereby acquiring suppressive actions over conventional T cells, themselves having an intermediate affinity toward self-peptides.[28–30] Peripheral Tregs (pTregs) develop separately induced from naïve peripheral CD4$^+$ T cells which acquire Foxp3 and CD25 expressing Treg functionality.[31–33] MLN-induced pTregs homing to the colonic mucosa are critical for oral tolerance,[9,34,35] but tTregs may act synergistically.[36,37] High-dose DSS is frequently used to model IBD, which also increases both MAMP-GALT contact and gut permeability.[38] Recently, DSS-induced IBD has been linked to thymic involution and changes in thymocyte subsets in mice,[39–41] suggesting a thymus–gut axis in which gut immune responses affect thymic T cell development. Thymic involution has previously been linked to, for example, pregnancy, glucocorticoid treatment, stress, and sepsis.[42–45]

We, therefore, hypothesized that reduced post-weaning mucosal integrity induced by a low dose of DSS in mice would cause increased gut permeability even if clinical colitis was absent and that this increase in the gut permeability would induce long-term gut regulatory immunity and central changes in thymocyte development, activation, and recruitment due to the direct thymic-gut axis.

## Materials and methods

The experiments were carried out in accordance with the EU Directive 2010/63/EU and approved by the Animal Experimentation Inspectorate, Ministry of Environment and Food, Denmark (license no. 2012-15-2934-00256).

### *Animals*

BALB/cAnNBomTac mice (Taconic, Lille Skensved, Denmark) were housed with aspen bedding (Tapvei/Brogaarden, Lynge, Denmark), Enviro-dri nesting material, cardboard shelters, Mini Fun Tunnel, and aspen chew blocks (Brogaarden, Lynge, Denmark) in open type 3 cages with wire lids (Tecniplast/Scanbur, Karlslunde, Denmark) at 21°C and lights on from 6 a.m. to 6 p.m., fed Altromin 1324 chow (Brogaarden) and watered with tap water except during study treatment periods.
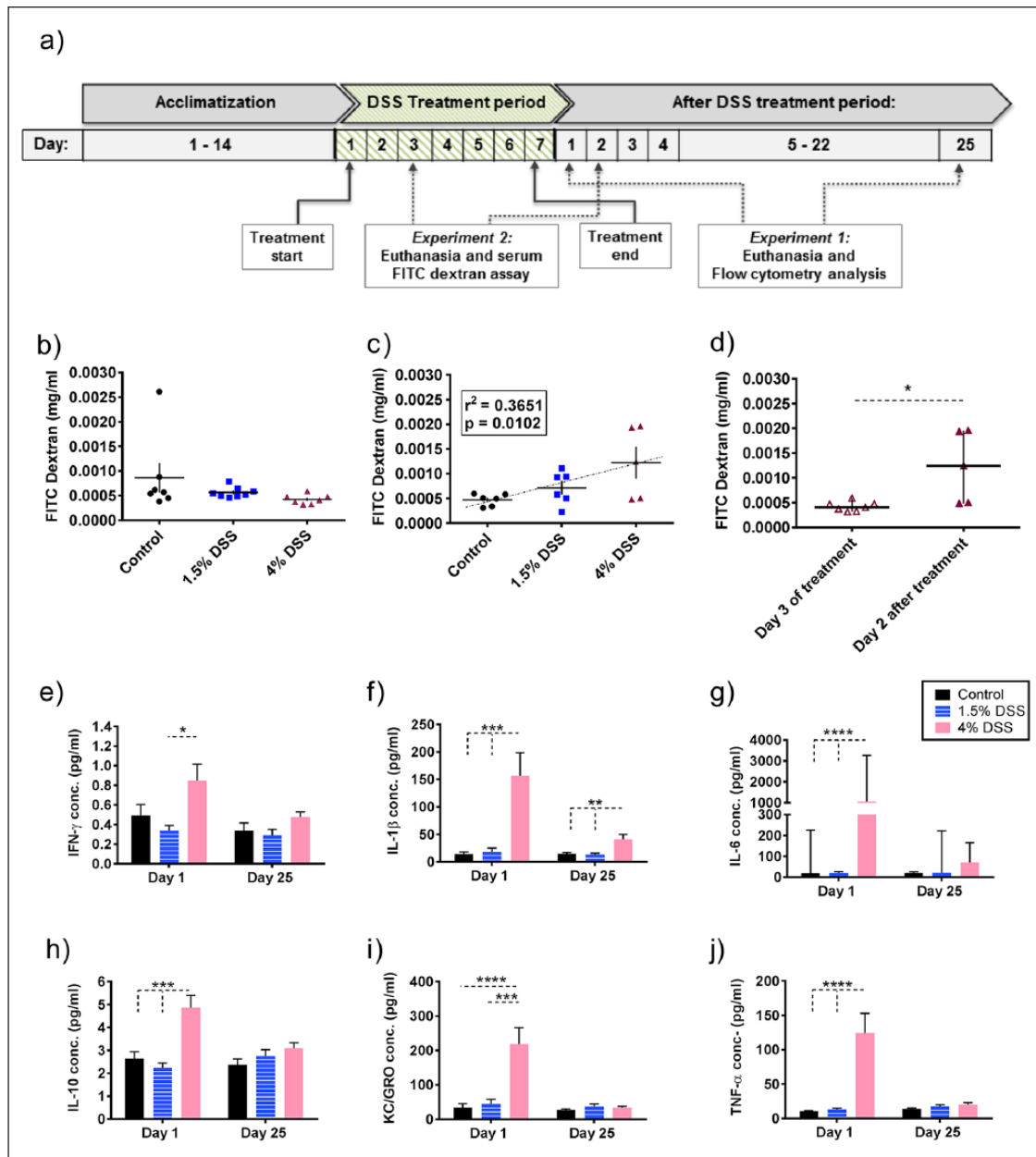
**Figure 1.** Effects of low- and high-dose dextran sulfate sodium (DSS) on gut permeability and cytokine expression in BALB/c mice (control, low dose (1.5%), and high dose (4%)). (a) Study timeline for Experiments 1 and 2. Serum FITC-Dextran concentrations on day 3 of treatment (b) and on day 2 after treatment (c), and for day 3 during treatment and day 2 after treatment in the high-dose groups (d). Mean colon cytokine concentrations IFN-γ (e), IL-1β (f), IL-6 (g), IL-10 (h), KC/GRO (i), and TNF-α (j) on day 1 (acute phase) and day 25 (long-term phase) after treatment. Group mean values and SEM are depicted on non-transformed data, except graphs (d) and (g) in which median and range are depicted due to non-Gaussian distribution of data. Graphs c, f, g, I, and j: statistics calculated on transformed data. Graph c: trend line for linear regression derived best fitted line depicted on graph (goodness of fit ($r^2$) and *P*-value (slope ≠ 0) in box). Graph d: significance levels as calculated with Mann–Whitney U test. *$P \leqslant 0.05$; ***$P \leqslant 0.001$; ****$P \leqslant 0.0001$.

## Experimental design

Two experiments were performed (Figure 1(a)) with females (Experiment 1) or mixed gender in a gender-blocked randomization (Experiment 2). In each experiment, animals were randomized into three treatment groups. Based on earlier treatment protocols[23,25,26,39,40,46] at 5 weeks of age, control group mice received regular tap water ad libitum throughout the experiment period, the low-dose group received 1.5% DSS (molecular weight of

36.000–50.000; MP Biomedicals, Santa Ana, CA, USA), while the high-dose group received 4% DSS in regular tap water ad libitum for 7 days (Experiment 1: n = 6–8/group per time point; Experiment 2: n = 7–8/group or n = 5–6/group on day 3 of treatment and day 2 after treatment, respectively, based on power calculation on previous data[23,25,26]). Body weight (BW), food, and water intake were registered weekly. Humane endpoints (>20% loss of BW and/or decreased general condition) were assessed daily during DSS treatment and the first 4 days after treatment, and hereafter, biweekly. Sacrifice time points were based on earlier studies.[40] In Experiment 1, half of the mice were euthanized by cervical dislocation on day 1 and day 25 after treatment for collecting samples during the acute inflammation phase and in the long-term phase after healing in the 4% group. In Experiment 2, half of the mice were euthanized by cervical dislocation on day 3 during treatment and day 2 after treatment to evaluate gut permeability during and after treatment. Before euthanasia, animals were anesthetized with fentanyl/fluanisone (Hypnorm; VetaPharma, Leeds, UK) and Midazolam (Dormicum, Roche, Denmark) diluted 1:1:2 in sterile water and retro-orbital blood samples were collected (Figure 1(a)).

### Clinical scoring

Clinical scoring[47,48] was performed to evaluate onset and extent of colon inflammatory development. Colon length (distal from the cecum to anal opening without fecal content) and colon weight/length ratio were determined to evaluate macroscopic colon changes from Experiment 1 mice. The disease activity index score to evaluate clinical colitis was determined for the 4% groups during treatment and the first 4 days after treatment. The score was based on daily evaluations of weight loss, stool consistency, occult blood in feces (Hemoccult SENSA; Beckman Coulter Inc., Atlanta, GA, USA), and general condition.[48]

### Histology

Distal colon samples (approximately 2 cm sagittal half) from Experiment 1 mice were stored in 9 mL S-Monovette® tubes, filled with 4% formaldehyde solution (Enclosed Formalin System; Sarstedt AG & Co, Nümbrecht, Germany) and processed for hematoxylin and eosin staining. Inflammation and crypt scores were blindly evaluated.[48] The sum of the crypt and inflammation scores was combined to a histological index score of microscopic pathology.

### Flow cytometry

MLN and thymus from Experiment 1 mice were stored in Eppendorf tubes containing 1 mL Hanks' balanced salt solution (Hanks') (A1711; AppliChem, St. Louis, MO, USA) at 5°C. Cells were isolated from the thymus and MLN shortly after organ collection by squeezing fresh organs between two microscope slides, resuspending in Hanks', and subsequently filtering through a 70-μm cell strainer. The total amounts of thymocytes were calculated after counting in a hemocytometer. The filtered cell suspensions were kept cold for the remainder of the preparation, centrifuged, and re-suspended in phosphate buffered saline (PBS) (Sigma-Aldrich, St. Louis, MO, USA) with 2% fetal bovine serum. Approximately, 4 million cells from each organ sample were transferred to a 96-well plate. Staining, for 30 min with surface marker antibodies, was used to distinguish different T cell populations. For nuclear staining of Foxp3 after surface staining, the cells were first fixated, permeabilized, and stained for intracellular Foxp3 according to the manufacturer's protocol (eBioscience, San Diego, CA, USA). The flow cytometry analysis was performed with BD LSRFortessa™ analyzer (BD Biosciences, Franklin Lakes, NJ, USA). The following mouse antibodies were utilized in the flow cytometry analysis: fluorescein isothiocyanate (FITC)-conjugated mAbs-recognizing CD103 (2E7) (eBioscience); phycoerythrin-conjugated mAbs-recognizing Foxp3 (FJK-16s; eBioscience); phycoerythrin-CF594-conjugaged mAbs-recognizing T cell receptor (TCR) γδ (GL3); phycoerythrin-cyanin7-conjugated mAbs-recognizing CD8α (53-6.7); Alexa Fluor 647–conjugated mAbs-recognizing CD218a (BG/IL-18RA); Alexa Fluor 600–conjugated mAbs-recognizing CD4 (RM4-5); Brilliant Violet 421–conjugated mAbs-recognizing CD314 (CX5; Biolegend, San Diego, CA, USA); allophycocyanin-cyanin7-conjugated mAbs-recognizing CD44 (IM7); Brilliant Violet 605–conjugated mAbs-recognizing CD3 (17A2); Brilliant Violet 711–conjugated mAbs-recognizing TCRβ (H57-597); and Brilliant Violet 786–conjugated mAbs-recognizing

CD25 (PC61); all antibodies were from BD Biosciences unless otherwise stated.

The output was analyzed with FlowJo v10 (Tree Star Inc., San Carlos, CA, USA) (detailed gating strategies in Supplemental Figures S1 and S2). Cells were stained for relevant identification markers and phenotypic markers: CD103, CD218a, CD314, CD44, and CD25. All cell samples were initially gated for size and removing of doublets (FSC-A/FSC-H). Time-axis gating removed air bubble interference in a few of the samples (eight MLN samples on day 1 after treatment, five MLN samples on day 25 after treatment, and one thymus sample on day 1 after treatment). The thymocyte sample was included in the percentage although excluded from the statistical analysis of the total number of thymus cells. Thymocytes were gated for CD4 and CD8α to identify different thymocyte subsets. SP CD4$^+$ TCRαβ$^+$ thymocytes and SP CD8$^+$ TCRαβ$^+$ thymocytes were identified. tTreg cells were identified from the SP CD4$^+$ TCRαβ$^+$ thymocyte population by their co-expression of Foxp3 and CD25. Finally, DN thymocytes were identified by lacking CD4, CD8α, TCRβ, and TCRγδ expression. Brilliant Violet 786 emission of the CD25-mAb in the DN population was too high to properly compensate. This was solved by adjusting the gating strategy to encompass the high emission. The DN1-DN4 subsets were further divided by their expression of CD25 and CD44; DN1 (CD25$^-$ CD44$^+$), DN1-2 (CD25$^{(int)}$ CD44$^+$), DN2 (CD25$^{(high)}$ CD44$^+$), DN3 (CD25$^+$ CD44$^-$), and DN4 (CD25$^-$ CD44$^-$). MLN cells were gated for TCRαβ and TCRγδ to identify TCRαβ$^+$ cells in the dump gate. CD8$^+$ TCRαβ$^+$ and CD8$^+$ TCRαβ$^+$ T cells were identified within the TCRαβ$^+$ gate. Foxp3$^+$ CD25$^+$ regulatory T cells and CD103$^+$ CD4$^+$ T cells were identified within the CD4$^+$ TCRαβ$^+$ gate, and finally, Foxp3$^+$ CD25$^+$ regulatory T cells within the CD103$^+$ CD4$^+$ TCRαβ$^+$ gate. The frequency of the lymphocyte gate was utilized to calculate the total thymocyte counts for each subset.

## Colon cytokine measurements

The distal colonic samples (approximately 2 cm distal sagittal half) from Experiment 1 mice were stored in sterile 1 mL Eppendorf tubes at −80°C until preparation. Colon pieces were prepared by defrosting and homogenizing with an Ultra Turrax T8 in cold inhibitor buffer (10 mg tissue to 100 μL buffer) consisting of MSD Tris Lysis buffer (cat. no. R60TX-3; MSD, Rockville, MD, USA) and enzyme inhibitors from the MSD inhibitor pack (cat. no. R70AA-1, MSD) (mix: 10 mL Tris lysis buffer; 100 μL phosphatase inhibitor 1; 100 μL phosphatase inhibitor 2; 200 μL protease inhibitor). After homogenization, the samples were left at 5°C in a refrigerator for 20 min, before centrifugation (7500 r/min, 5 min, 5°C), removal of the supernatant to clean Eppendorf tubes and storage at −80°C until the inflammatory cytokines interferon (IFN)-γ, IL-10, IL-12p70, IL-1β, IL-2, IL-4, IL-5, IL-6, keratinocyte chemoattractant/growth-regulated oncogene (KC/GRO), and tumor necrosis factor (TNF)-α, were measured with the V-PLEX Proinflammatory Panel 1 (mouse) Kit multiplex immunoassay (cat. no. K15048D-2, MSD), as recommended by the manufacturer. All plates were analyzed utilizing a Sector Imager (MSD).

## FITC-Dextran assay

FITC-Dextran (average molecular weight: 3000–5000; Sigma-Aldrich) was dissolved in PBS (Sigma-Aldrich) with 125 mg/mL. Experiment 2 mice were fasted 6 h and gavaged with FITC-Dextran (600 mg/kg). Precisely 2 h after dosing, retro-orbital blood samples were collected into sterile Eppendorf tubes using sodium heparin hematocrit tubes. Blood samples were centrifuged (4°C, 8000$g$, 7 min), and serum was transferred to clean Eppendorf tubes and diluted 1:1 with PBS. Two independent standard curves were prepared by utilizing diluted serum (1:1 with PBS) from PBS sham dosed (orally) mice. Stock FITC-Dextran (125 mg/mL) was mixed in diluted serum to a concentration of 0.008 mg/mL and serially diluted 1:2 with diluted serum to a concentration of $1.25 \times 10^{-4}$ mg/mL. Pure diluted serum was utilized as a zero concentration. Samples were plated in 100 μL triplets or duplets, and standard curves were plated on a black 96-well microplate. The concentration of FITC-Dextran in serum was determined by a spectrophotometric fluorometry plate reader (excitation 485 nm, emission wavelength 535 nm).

## Statistics

All rawdata output from experiments used for statistical analysis can be found in supplementary table 5. Normality and variances were evaluated with d'Agostino–Pearsson test, Brown–Forsythe test, or F-test. Parametric data were achieved by transformations when appropriate, and differences between group mean values evaluated with one-way analysis of variance (ANOVA) with Tukey's multiple comparisons or Student's t-test with $P$-values $\geqslant 0.05$ considered significant. Non-parametric data were evaluated with Kruskal–Wallis along with Dunn's multiple comparisons test, or the Mann–Whitney U test. Correlations between the DSS treatment doses and thymocytes or MLN T cells were analyzed with linear regression if observing trends of a dose correlation. Four MLN cell samples (one in 1.5% DSS group and three in 4% DSS group, day 1 after treatment) were excluded from statistical analysis due to extensive cell death.

## Results

### DSS increased gut permeability and induced an inflammatory state without morphological colitis in the low-dose (1.5%) group

On day 2 after treatment, FITC-Dextran assay, during and shortly after DSS treatment, showed a linear positive dose response in gut permeability (Figure 1(b)–(d)). The combination of the histological index, colon length, and weight/length ratio did not indicate macroscopic or microscopic colitis in the 1.5% group at any time, apart from a significantly lower colon length than the control group on day 1 after treatment ($P \leqslant 0.05$). Colitis was observed in the 4% group acute on day 1 after treatment, as the histological index, colon length, and weight/length all differed significantly from the control group ($P \leqslant 0.0001$; $P \leqslant 0.01$; and $P \leqslant 0.0001$, respectively), as known for acute colitis.[46] On day 25 after treatment, a chronic colitic state was still observed in the 4% group with a significantly higher histological index than the control group ($P \leqslant 0.05$). The disease activity index score indicated that clinical colitis started on day 5 during treatment with symptom severity increasing until day 2 after treatment, whereafter it started subsiding. BW, food intake, and water intake

registrations correlated with the clinical scoring (Supplemental Figures S3 and S4).

### Cytokine responses in the low-dose (1.5%) group were comparable to the control group

In the 1.5% group, no cytokine levels differed significantly from the control group at any time. The levels of pro-inflammatory cytokines in the 4% group IL-1β ($P \leqslant 0.001$), IL-6 ($P \leqslant 0.0001$), TNF-α ($P \leqslant 0.0001$), IL-10 ($P \leqslant 0.001$), and KC/GRO ($P \leqslant 0.001$) were significantly higher in the colon compared to both other groups on day 1 after treatment (Figure 1(e)–(j)), which is comparable to other studies.[46,49–51] Furthermore, IFN-γ was significantly higher in the 4% group on day 1 after treatment compared to the 1.5% group ($P \leqslant 0.05$). As the significant differences in both IFN-γ and IL-10 between the dosing groups were small, these may have less biological relevance. Compared to day 1 after treatment, all above-mentioned cytokines reduced significantly in the 4% group on day 25 after treatment (IFN-γ, $P \leqslant 0.05$; IL-6, $P \leqslant 0.01$; IL-10, $P \leqslant 0.05$; KC/GRO, $P \leqslant 0.0001$; and TNF-α, $P \leqslant 0.001$), with exception of IL-1β, which remained significantly higher compared to both the other groups on day 25 after treatment (both $P \leqslant 0.01$). IL-5 and IL-12p70 concentrations did not differ between groups at any time.

### Increased permeability caused mild generalized acute thymic involution

To evaluate thymocyte differentiation changes and possible thymic involution, the total number of thymocytes and all major subsets were estimated and analyzed. A general trend showed a mild degree of acute thymic involution on day 1 after treatment in both cortical and medullary subsets of the thymus and a negative correlation between DSS dose and the total number of thymocytes (Figure 2(a)).

Thymocyte subset distribution was similarly indicating the same stress level in all three groups (Figure 2(b)–(d)). The thymic involution on day 1 after treatment was mirrored in early developmental DN1, DN1-2, DN3, and DN4 thymocyte subsets displaying linear negative dose responses, which all were significantly lower in the 4% group compared to the control group (all $P \leqslant 0.01$). A lower amount of thymocytes in the DN1, DN1-2,
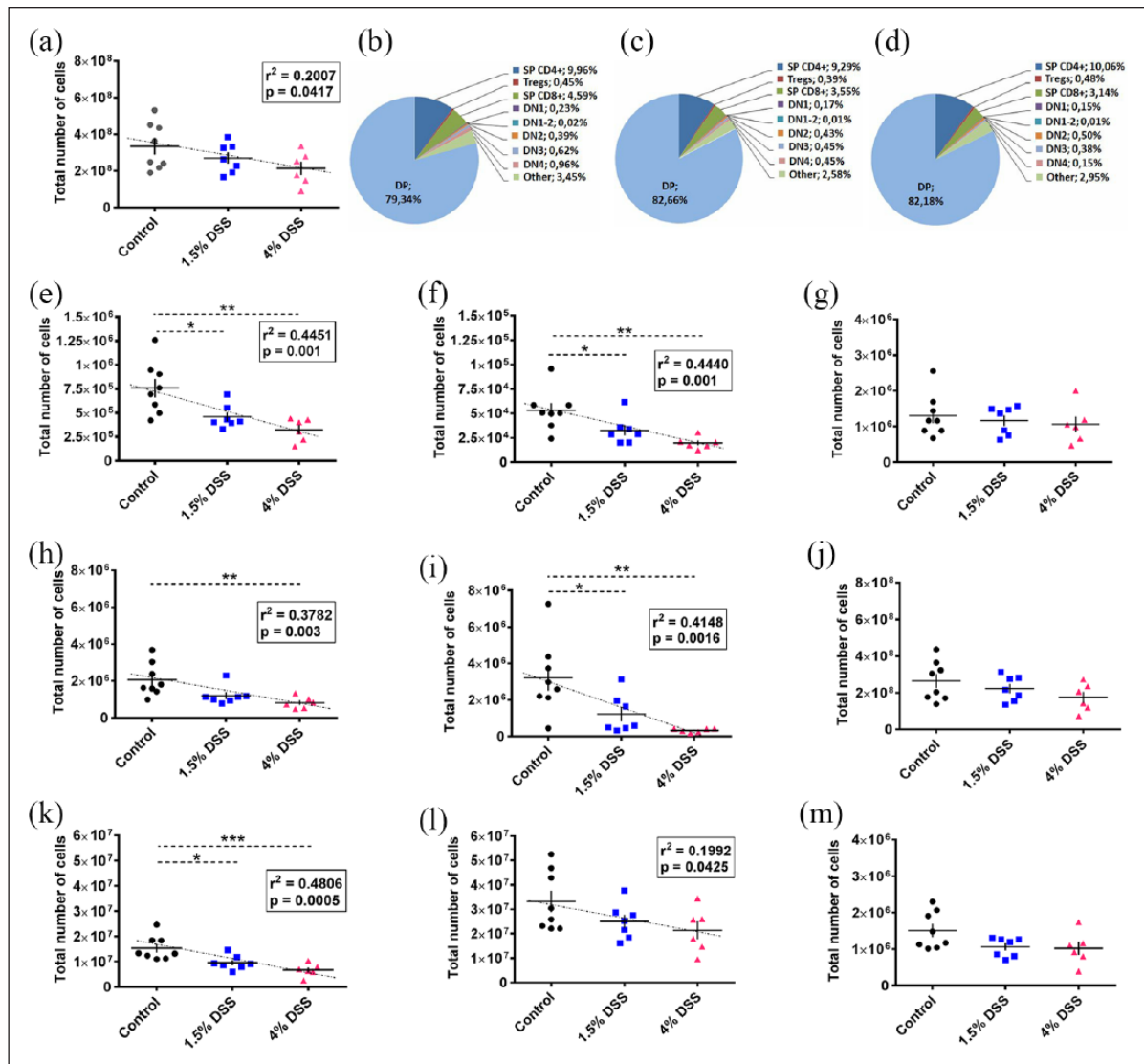
**Figure 2.** Thymocyte counts after low-dose (1.5%) and high-dose (4%) dextran sulfate sodium (DSS) treatment in BALB/c mice. (a) Total thymocyte count on day 1 after treatment. Thymocyte subset distribution day 1 after treatment for the control group (b), the 1.5% group (c), and the 4% group (d). Total thymocyte counts in the three treatment groups on day 1 after treatment for the thymocyte subsets double negative (DN1) (e), DN1-2 (f), DN2 (g), DN3 (h), DN4 (i), DP (j), single positive (SP) CD8+ (k), SP CD4+ (l), and Foxp3+ CD25+ regulatory T cells (Tregs) (m). Group mean values and SEM are depicted on non-transformed data. Trend line for linear regression derived best fitted line depicted on graphs if significant (Goodness of fit ($r^2$) and *P*-value (slope $\neq$ 0) in box).
*$P \leqslant 0.05$; **$P \leqslant 0.01$; ***$P \leqslant 0.001$.

and DN4 subsets was also observed between the control and 1.5% groups (all $P \leqslant 0.05$) (Figure 2(e), (f), (h), and (i)). Apart from a general trend of negative linear dose-response, there were no single linear correlations or significant differences in the DN2 or DP thymocyte subsets on day 1 after treatment (Figure 2(g) and (j)). Significantly less mature SP CD8+ subset thymocytes were found in both the 1.5% and 4% groups compared to the control

group ($P \leqslant 0.05$ and $P \leqslant 0.001$, respectively). Both SP CD4+ and SP CD8+ thymocyte displayed linear negative dose responses, but no significant differences were found between groups in the mature SP CD4+ thymocytes indicating a stronger impact on the SP CD8+ subset (Figure 2(k) and (l)). Finally, no significant correlations or differences were found in the total thymocyte counts of the Foxp3+ CD25+ Treg thymocytes (Figure 2(m)).
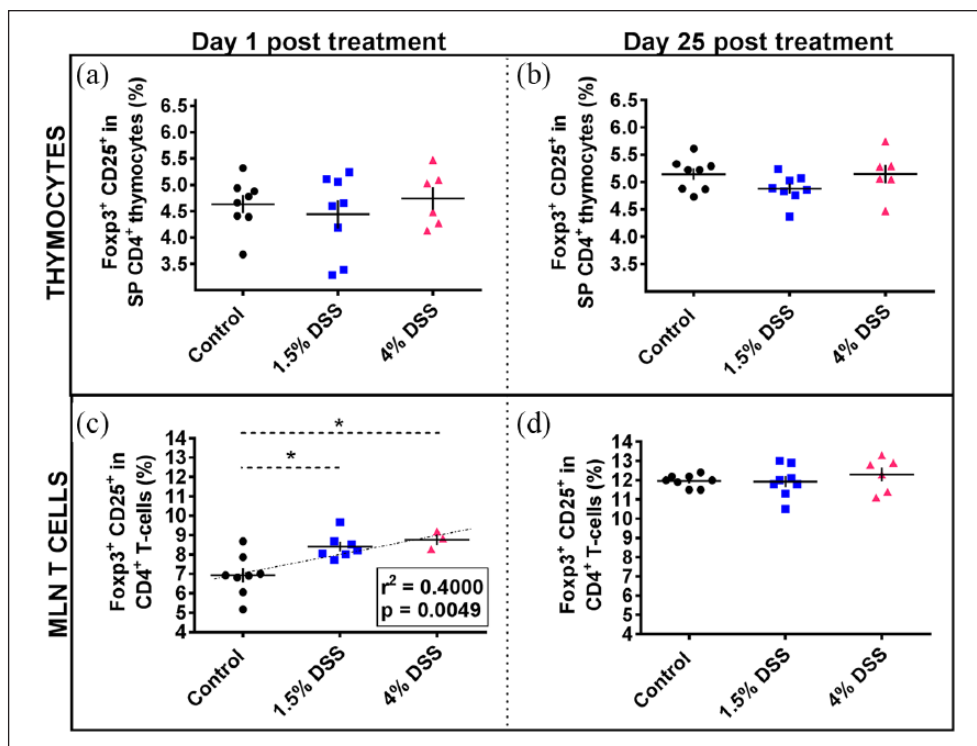
**Figure 3.** Foxp3 expression on thymus and mesenteric lymph node (MLN) T cells after low-dose (1.5%) and high-dose (4%) dextran sulfate sodium (DSS) treatment in BALB/c mice. Co-expression (%) of regulatory T cell (Treg) markers Foxp3 and CD25 on single positive (SP) CD4+ thymocytes day 1 (a) and day 25 after treatment (b). Co-expression (%) of Treg markers Foxp3 and CD25 on CD4+ T cells in the MLN on day 1 (c) and day 25 after treatment (d). Group mean values and SEM are depicted on non-transformed data. Trend line for linear regression derived best fitted line depicted on graphs if significant (goodness of fit ($r^2$) and $P$-value (slope $\neq$ 0) in box).
*$P \leqslant 0.05$.

Interestingly, a reversal of the acute thymus involution was observed with no differences in counts of total thymocytes of individual subsets between treatment groups on day 25 after treatment.

### Increase in the permeability increased Foxp3+ CD25+ Treg cell numbers transiently in the MLNs, but not in the thymus

Analyzing the frequencies of Foxp3 and CD25 co-expression on SP CD4+ thymocytes and MLN CD4+ T cells showed that in the thymus Foxp3+ CD25+ tTreg, cells were relatively unaffected by the treatment (Figure 3(a) and (b)). In the MLN, the Foxp3+ CD25+ Treg cells showed a linear positive dose response on day 1 after treatment, and the expression in the 1.5% and 4% groups was significantly higher compared to the control group (both $P \leqslant 0.05$). The effects were absent on day 25 after treatment, indicating a normalization of the cell population homeostasis at this time point in the MLN (Figure 3(c) and (d)).

### Increase in the permeability changed thymocyte and MLN T cell gut-homing

To assess how DSS treatment changes gut-homing, CD103 expression[52–55] was analyzed on the different thymocyte and MLN T cell subsets. CD103+ SP CD8+ thymocytes expressed a linear positive dose-related response on day 1 after treatment, however without significant differences between groups (Figure 4(a)).

Conversely, the CD103+ DN2 thymocytes expressed a linear negative dose-response on day 1 after treatment with small but significantly lower expression in the 1.5% and 4% groups compared to the control group ($P \leqslant 0.01$ and $P \leqslant 0.001$, respectively) (Figure 4(d)). MLN CD4+ T cells expressed a minor but significant ($P \leqslant 0.05$) increase in the CD103 from 1.97% in the control group to 2.36% in the 1.5% group on day 1 after treatment (Figure 4(f)). As most CD103 expressing CD4+ T cells also expressed Foxp3 and CD25 (mean group expressions between 72.59% and
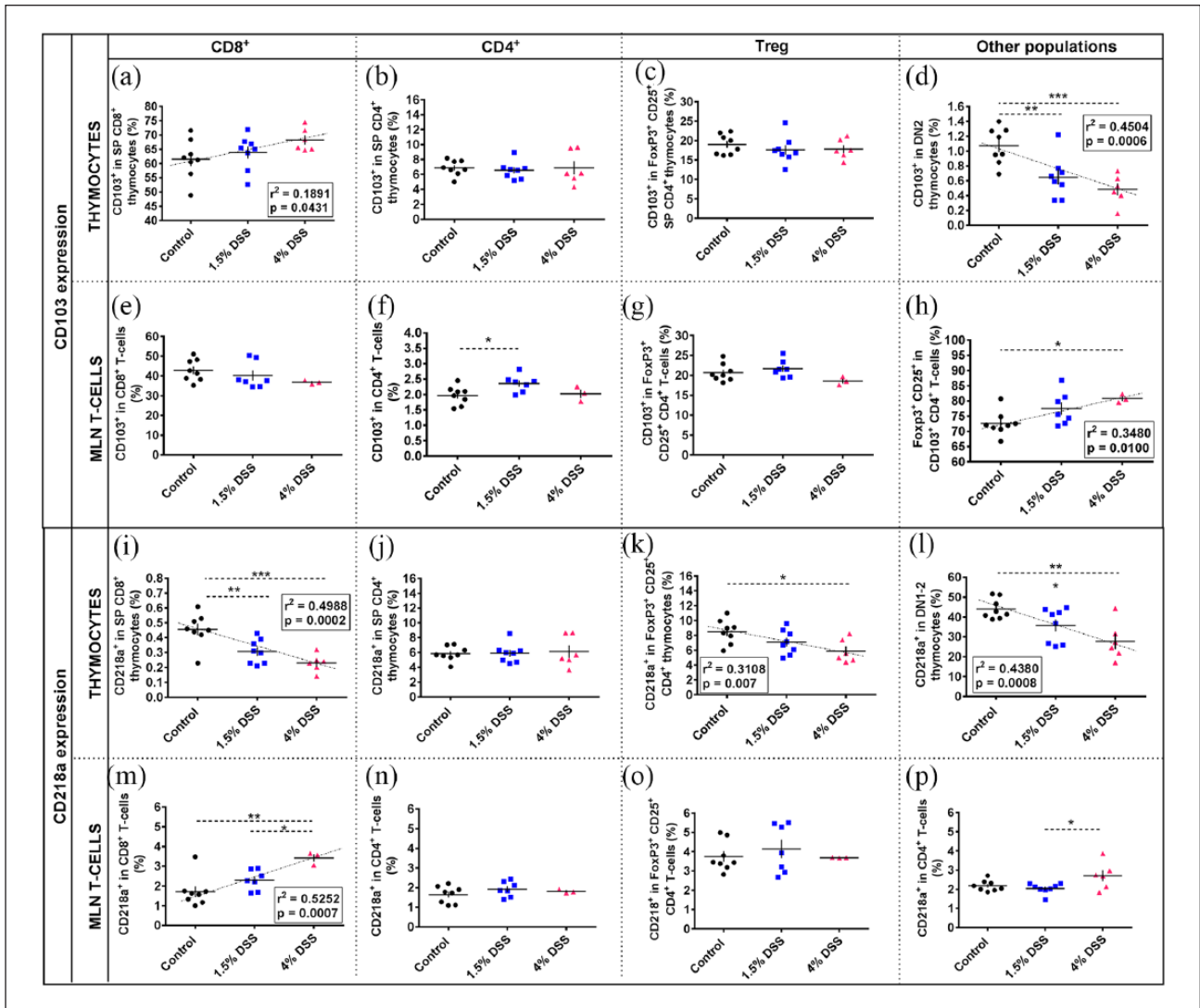
**Figure 4.** Gut-homing and activation marker expression on thymocyte and mesenteric lymph node (MLN) T cell subsets after low-dose (1.5%) and high-dose (4%) dextran sulfate sodium (DSS) treatment in BALB/c mice. The CD103 expression (%) is depicted in the single positive (SP) CD8+ (a), SP CD4+ (b), Foxp3+ CD25+ regulatory T cells (Treg) (c), and double negative (DN2) (d) thymocyte subsets day 1 after treatment. The CD218a expression (%) is depicted in the SP CD8+ (i), SP CD4+ (j), Treg (k), and DN1-2 (l) thymocyte subsets day 1 after treatment. The CD103 expression (%) is depicted in the CD8+ (e), the CD4+ (f), and the Treg (g) MLN T-cell subsets, and co-expression (%) of Foxp3 and CD25 is also depicted on the CD103+ CD4+ (h) MLN T cells on day 1 after treatment. The CD218a expression (%) is depicted in the CD8+ (m), the CD4+ (n), and the Treg (o) MLN T cells on day 1 after treatment, and in the CD4+ MLN T cells on day 25 after treatment (p). Group mean values and SEM are depicted on non-transformed data in each graph. Trend line for linear regression derived best fitted line depicted on graphs if significant (goodness of fit ($r^2$) and $P$-value (slope $\neq$ 0) in box).
*$P \leqslant 0.05$; **$P \leqslant 0.01$; ***$P \leqslant 0.001$.

80.77%), the majority of the gut-homing CD4+ T cells were Tregs. Furthermore, a linear positive dose response in the co-expression of the Treg cell markers Foxp3 and CD25 was found on the subset. Significantly higher co-expression of Foxp3 and CD25 Treg cell markers on gut-homing CD4+ T cells in the 4% group compared to the control group on day 1 after treatment ($P \leqslant 0.05$) was also observed. Overall, this indicates an increase in the Tregs in the gut-homing CD4+ T cell subset of the MLN (Figure 4(h)). No other changes in CD103+ expression were observed on any thymocyte or MLN T cell subset at any time point.

*Increase in the permeability changed activation of several thymocytes subsets and T cell subsets in MLN*

To assess how DSS treatment changed activation, the marker CD218a and the co-stimulatory marker CD314[56–58] were analyzed on the different thymocyte and MLN T cell subsets. SP CD8^{+} thymocytes, Foxp3^{+} CD25^{+} tTregs, and the DN1-2 subsets expressed a negative linear dose response of CD218a. On day 1 after treatment, a significant reduction in CD281a expression was observed for all three subsets in the 4% group compared to the control group ($P \leqslant 0.001$, $P \leqslant 0.05$, and $P \leqslant 0.01$, respectively). A similar reduction was observed for the SP CD8^{+} thymocytes in the 1.5% group compared to the control group ($P \leqslant 0.01$). Relatively small decreases in the CD218a expression were observed on SP CD8^{+} thymocytes and Foxp3^{+} CD25^{+} tTregs. However, a relatively large decrease from a mean expression of 44.13% in controls to 27.73% in the 4% group was observed in the DN1-2 subset (Figure 4(i), (k), and (l)). At no time point were changes in CD218a expression observed on the SP CD4^{+} (Figure 4(j)) or other thymocyte subsets. Interestingly, in the MLN T cells, a linear positive dose response was observed in the CD218a expression on CD8^{+} T cells on day 1 after treatment, along with significantly higher expression in the 4% group compared to the control and 1.5% groups ($P \leqslant 0.01$ and $P \leqslant 0.05$, respectively). No differences in CD218a expression were observed in the CD4^{+} T cells or Foxp3^{+} CD25^{+} Treg cells of the MLN on day 1 after treatment (Figure 4(m)–(o)). Interestingly, the MLN CD4^{+} T cells of the 4% group expressed significantly more CD218a compared to the 1.5% group on day 25 after treatment, indicating a delayed response (Figure 4(p)). The increased activation of MLN CD8^{+} T cells on day 1 after treatment was also observed as a positive dose response in expression of the co-stimulatory marker CD314 ($r^2 = 0.3356$, $P \leqslant 0.05$) along with minor but significantly higher expression in the 4% (0.47%) compared to the control group (0.15%) ($P \leqslant 0.05$). A positive linear dose response in CD314 expression was also observed in the MLN CD4^{+} T cells ($r^2 = 0.3553$, $P \leqslant 0.01$) and Treg T cells ($r^2 = 0.2787$, $P \leqslant 0.05$), along with significantly increased expression in the 4% compared to the control groups ($P \leqslant 0.05$) of

CD4^{+} T cells. Furthermore, a positive dose response in CD25 and CD44 expression on CD4^{+} T cells in the MLN ($r^2 = 0.4270$, $P \leqslant 0.01$) was observed on day 1 after treatment along with significantly increased expression in both the 1.5% and the 4% groups compared to the control group ($P \leqslant 0.01$ and $P \leqslant 0.05$, respectively). No other relevant differences between groups were found on any thymocyte subsets or MLN T cell subsets on day 1 or day 25 after treatment.

*Changed CD103 and CD218a expressions are correlated to reduced total thymocyte counts*

The total amount of SP CD8^{+} and DN2 thymocytes expressing CD103 and the amounts of SP CD8^{+}, Treg, and DN1-2 thymocytes expressing CD218a on day 1 after treatment were analyzed to evaluate if changed expression of these markers were also reflected in the total thymocyte counts (Table 1). A negative dose response was found in the total thymocyte counts of CD103 expressing SP CD8^{+} and DN2 thymocyte subsets on day 1 after treatment, as reflected by significantly decreased counts in the 4% groups compared to the control group for both subsets ($P \leqslant 0.01$ and $P \leqslant 0.05$, respectively). There were significantly fewer CD103^{+} expressing DN2 thymocytes in the 1.5% compared to the control group ($P \leqslant 0.05$). A ROUTs test (Q = 1%) identified outlier (with a total thymocyte count of 1,440,000) was removed from the control group when analyzing the CD103^{+} DN2 subset. The total thymocyte counts of CD218a expressing SP CD8^{+}, tTreg, and DN1-2 thymocytes were all significantly decreased compared to the control group in both the 1.5% group ($P \leqslant 0.01$, $P \leqslant 0.01$, and $P \leqslant 0.05$, respectively) and the 4% group ($P \leqslant 0.001$, $P \leqslant 0.01$, and $P \leqslant 0.001$, respectively). Negative dose responses were also identified for all three subsets. This shows that DSS decreases the number of thymocytes expressing CD218a.

## Discussion

As previously described,[23,25,26] post-weaning oral DSS treatment increased gut permeability in mice. While active colitis was absent in the 1.5% group, the 4% dose induced both macroscopic and microscopic acute colitis, and acute pro-inflammatory cytokine increases indicative of an immune

**Table 1.** Total thymocyte counts for selected subsets on day 1 after dextran sulfate sodium (DSS) treatment in BALB/c mice.

| Thymocyte subset | Mean (SD) ($10^6$ thymocytes) | | | Linear regression | | |
|---|---|---|---|---|---|---|
| | Control group | 1.5% DSS group | 4% DSS group | Slope ± SE ($10^6$ cells) | $r^2$ | *P*-value |
| CD103$^+$ single positive CD8$^+$ | 9.477$^c$ (3.270) | 6.289 (1.922) | 4.547$^a$ (1.695) | −1.208 ± 0.338 | 0.4018 | 0.0020 |
| CD103$^+$ double negative 2 | 0.015$^{b,c}$ (0.008) | 0.007$^a$ (0.003) | 0.005$^a$ (0.003) | −0.002 ± 0.001 | 0.3071 | 0.0112 |
| CD218a$^+$ single positive CD8$^+$ | 0.071$^{b,c}$ (0.030) | 0.030$^a$ (0.014) | 0.016$^a$ (0.006) | −0.013 ± 0.003 | 0.5127 | 0.0003 |
| CD218a$^+$ regulatory T cell | 0.127$^{b,c}$ (0.043) | 0.070$^a$ (0.012) | 0.058$^a$ (0.020) | −0.017 ± 0.004 | 0.4353 | 0.0011 |
| CD218a$^+$ double negative 1–2 | 0.023$^{b,c}$ (0.009) | 0.012$^a$ (0.007) | 0.006$^a$ (0.003) | −0.004 ± 0.001 | 0.5046 | 0.0003 |

$^a$*P* < 0.05 versus control group.
$^b$*P* < 0.05 versus low-dose group (1.5% DSS group).
$^c$*P* < 0.05 versus high-dose group (4% DSS group).

response due to increased microbial antigen burdens.[46,49,50] This progressed to chronic pathology with CD218a expression on CD4$^+$ T cells and a persisting increase in the colon levels of IL-1β, as known for colitis.[59–61] DSS treatment increased gut permeability, which as hypothesized induced a short-term generalized thymic involution in both groups. tTregs resisted the thymic involution, but the changed expression of gut-homing marker CD103 on mature SP CD8$^+$ and DN2 thymocytes along with CD4$^+$ MLN T cells indicated acute cell mobilization to the gut. Activation expressed by CD218a was found to acutely decrease on SP CD8$^+$, Tregs, and DN1-2 thymocytes while simultaneously increasing on MLN CD8$^+$ T cells. The overall similar relative thymocyte subset distribution in all three groups indicates that changes observed were DSS-induced and not a stress-induced thymic involution.

Acute colitis has previously been linked to thymic involution,[39,41,62] and it has been suggested to lead to a combination of both increased thymocyte apoptotic rates and increased T cell release to the periphery.[41,63,64] We show that thymic involution occurs even in the lack of colon inflammation. Interestingly, we found that different thymocyte populations seem to respond differently to gut signals with a more pronounced decrease in the SP CD8$^+$ compared to SP CD4$^+$ thymocytes. This suggests that an increased GM–host contact acutely leads to a higher migration of naïve CD8$^+$ T cells than CD4$^+$ T cells to the gut, which may also be an indication of increased GM–host contact.[65] The observed changes in functional traits of both medullary and cortical thymocyte subsets may indicate increased naïve T cell release from the thymus to the periphery due to increased permeability and GM-host interaction. The gut-homing marker

CD103 plays a functional role in thymocyte development,[66] and the increase in the CD103 expression on SP CD8$^+$ thymocytes might reflect expanded proliferation and naïve CD8$^+$ T cell release to the periphery.[67] Acutely increased CD103 expression on SP CD8$^+$ thymocytes along with decreased numbers of the subset could, therefore, indicate increased proliferation and CD8$^+$ T cell release. Some commercial barrier bred mice lack CD8$^+$ T cells,[68] which in the light of our findings may be due to the lacking early life bacterial stimulation. Peaudecerf et al.[69] showed that unconventional intraepithelial lymphocytes (IELs) are able to leave the thymus during the DN1-2 and DN2 stage of thymus development via an alternative pathway. As both the CD103 expression level on DN2 thymocytes and total numbers of the subset were acutely decreased, this could indicate at a peripheral release of these thymocytes, potentially via this alternative pathway, to the gut intraepithelial lymphocyte compartment. However, more studies are needed to investigate if this is a DSS/gut-specific phenomenon.

Activated CD218a expressing thymocytes in vitro and in vivo can be stimulated with IL-12 and IL-18 to increase apoptotic rates and production of IFN-γ.[70] Across several thymocyte subsets, such as SP CD8$^+$, DN1-2, and Treg thymocytes, decreased CD218a expression was observed during acute thymic involution. The decreased CD218a expression on SP CD8$^+$ thymocytes along with decreased numbers of this subset coinciding with an increase in the marker expression on CD8$^+$ T cells in the MLN is especially interesting, as this may point at an increased release of CD218a expressing thymocytes to the periphery rather than involution due to increased apoptosis. Future studies may determine whether CD218a is a potential marker for thymic

involution and whether CD218a expression on SP CD8^{+}, DN1-2, and Treg thymocytes is associated with gut immune responses. Although our study cannot reject a role of thymocyte apoptosis after DSS treatment, it indicates increased release of thymic CD218a^{+} CD8^{+} T cells migrating to the MLN, which again indicates a possible direct link between the thymus and MLN as a response to increased GM–host contact.

As the increased gut permeability only seemed to increase Foxp3^{+} CD25^{+} Treg numbers in the MLNs while not in the thymus, the MLN Foxp3^{+} CD25^{+} Treg increase may be due to increased induction of Foxp3^{+} CD25^{+} pTregs rather than migration of Foxp3^{+} CD25^{+} tTregs. Interestingly, increased gut permeability and the assumed subsequently increased GM–host contact seemed to increase the relative amount of Foxp3^{+} CD25^{+} Tregs in the gut-homing MLN CD103^{+} CD4^{+} T cell subset. As no increase in CD103 expression was observed in MLN Tregs, de-novo-synthesized pTregs may be mobilized rather than existing MLN Tregs. Furthermore, a relatively small but significant increase in the gut-homing marker CD103 expression on MLN CD4^{+} T cells was also observed in mice treated with low-dose DSS, that is, increased GM–host contact does induce an immunological response in which MLN CD4^{+} T cells and Foxp3^{+} CD25^{+} Tregs acutely home to the gut. The lack of a clear Foxp3^{+} CD25^{+} tTreg response suggests that the homeostatic regulation of immune responses in the gut taking part from day to day is primarily handled by the MLN T cell pool and proliferation of already gut-associated tTregs.

The lack of long-term effects suggests that the MLN regulatory responses are not maintained by high cell numbers or cytokine signals, and accordingly, most interventions in the GM of mice resulting in permanently altered immunity have been performed during fetal life or in pre-weaning pups.[13,16] Also intervention right after weaning induces a permanent immune modulation, implicating that the post-weaning phase is also important for immune system development.[15] Taken together, the above described results could narrow down the window for permanent immune modulation to the postnatal period including the immediate days after weaning. This is also the period when the immune system encounters a large load of unknown antigens. Another influencing factor for long-term immune modulation

might be how DSS treatment itself affects GM composition. A 1.5% DSS treatment in 5-week-old mice induces a loss of species diversity, and it favors Gram-negative phyla acutely from day 1 after treatment and long term to day 25 after treatment.[23,71,72]

Increased GM–host contact seems to induce some acute MLN adaptive responses as indicated by the increased expression of CD44, CD25, and CD314 on CD4^{+} T cells as well as CD218a and CD314 acutely on CD8^{+} T cells.[4,73–75] We also observed long-term induction of CD218a on CD4^{+} T cells in the MLN in the 4% group. Earlier studies have shown that intestinal wall CD218a^{+} CD4^{+} T cells, which may be stimulated to release pro-inflammatory cytokines, are present in lymphoid aggregates of human Crohn's disease patients, and in both human and mice, CD218a expressing CD4^{+} T cells are disposed to secrete IFN-γ if stimulated with IL-18.[76,77] A possible mechanism could be less rigid thymic thymocyte selection processes, due to processes being accelerated by an increased peripheral T cell need during active gut inflammation. This is supported by a study finding that colitis-derived thymic involution leads to negative selection failure, increasing the number of auto-reactive T cells in the periphery and inducing a chronic inflammatory phenotype predisposing for autoimmune diseases.[78] The observed increase in the relative fraction of mature SP thymocyte subsets may further support this.[39,41]

In conclusion, this study demonstrated that low-dose DSS treatment in post-weaning 5-week-old BALB/c mice even in the absence of high-grade inflammation increased gut permeability leading to non-persisting generalized thymic involution including most thymocyte subsets. Also, acute and non-persisting MLN regulatory responses were induced as a relative increase in the Foxp3^{+} CD25^{+} Tregs in the gut-homing marker expressing CD4^{+} T cell pool. We showed no changes in total thymic Foxp3^{+} CD25^{+} tTreg thymocyte numbers, and thus, the thymus does not seem to play a major role in post-weaning GM–host contact induced regulatory immunity, which in our study primarily was located to the gut.

## Supplemental material

Supplemental material for this article is available online.

## ORCID iD

Hannah Louise Zakariassen  https://orcid.org/0000 -0003-4792-3948

## References

1. Bendtsen KM, Fisker L, Hansen AK et al. (2015) The influence of the young microbiome on inflammatory diseases—Lessons from animal studies. *Birth Defects Research. Part C, Embryo Today* 105: 278–295.
2. Strachan DP (1989) Hay-fever, hygiene, and household size. *British Medical Journal* 299: 1259–1260.
3. Weng M and Walker WA (2013) The role of gut microbiota in programming the immune phenotype. *Journal of Developmental Origins of Health and Disease* 4: 203–214.
4. Sakaguchi S, Sakaguchi N, Asano M et al. (1995) Immunologic self-tolerance maintained by activated T cells expressing IL-2 receptor alpha-chains (CD25). Breakdown of a single mechanism of self-tolerance causes various autoimmune diseases. *Journal of Immunology* 155: 1151–1164.
5. Suri-Payer E, Amar AZ, Thornton AM et al. (1998) CD4+CD25+ T cells inhibit both the induction and effector function of autoreactive T cells and represent a unique lineage of immunoregulatory cells. *Journal of Immunology* 160: 1212–1218.
6. Fontenot JD, Gavin MA and Rudensky AY (2003) Foxp3 programs the development and function of CD4+CD25+ regulatory T cells. *Nature Immunology* 4: 330–336.
7. Hori S, Nomura T and Sakaguchi S (2003) Control of regulatory T cell development by the transcription factor Foxp3. *Science* 299: 1057–1061.
8. Khattri R, Cox T, Yasayko SA et al. (2003) An essential role for Scurfin in CD4+CD25+ T regulatory cells. *Nature Immunology* 4: 337–342.
9. Dubois B, Chapat L, Goubier A et al. (2003) Innate CD4+CD25+ regulatory T cells are required for oral tolerance and inhibition of CD8+ T cells mediating skin inflammation. *Blood* 102: 3295–3301.
10. Kuhn R, Lohler J, Rennick D et al. (1993) Interleukin-10-deficient mice develop chronic enterocolitis. *Cell* 75: 263–274.
11. Maynard CL, Harrington LE, Janowski KM et al. (2007) Regulatory T cells expressing interleukin 10 develop from Foxp3+ and Foxp3- precursor cells in the absence of interleukin 10. *Nature Immunology* 8: 931–941.
12. Williams AM, Probert CSJ, Stepankova R et al. (2006) Effects of microflora on the neonatal development of gut mucosal T cells and myeloid cells in the mouse. *Immunology* 119: 470–478.
13. Olszak T, An DD, Zeissig S et al. (2012) Microbial exposure during early life has persistent effects on natural killer T cell function. *Science* 336: 489–493.
14. Salminen S, Endo A, Isolauri E et al. (2015) Early gut colonization with Lactobacilli and Staphylococcus in infants: The hygiene hypothesis extended. *Journal of Pediatric Gastroenterology and Nutrition* 62: 80–86.
15. Hansen CHF, Nielsen DS, Kverka M et al. (2012) Patterns of early gut colonization shape future immune responses of the host. *PLoS ONE* 7: e34043.
16. Russell SL, Gold MJ, Willing BP et al. (2013) Perinatal antibiotic treatment affects murine microbiota, immune responses and allergic asthma. *Gut microbes* 4: 158–164.
17. Derrien M, Collado MC, Ben-Amor K et al. (2008) The Mucin degrader *Akkermansia muciniphila* is an abundant resident of the human intestinal tract. *Applied and Environmental Microbiology* 74: 1646–1648.
18. Hanninen A, Toivonen R, Poysti S et al. (2017) *Akkermansia muciniphila* induces gut microbiota remodelling and controls islet autoimmunity in NOD mice. *Gut* 67: 1445–1453.
19. Hansen CHF, Krych L, Nielsen DS et al. (2012) Early life treatment with vancomycin propagates *Akkermansia muciniphila* and reduces diabetes incidence in the NOD mouse. *Diabetologia* 55: 2285–2294.
20. Png CW, Linden SK, Gilshenan KS et al. (2010) Mucolytic bacteria with increased prevalence in IBD mucosa augment in vitro utilization of mucin by other bacteria. *American Journal of Gastroenterology* 105: 2420–2428.
21. Wang L, Christophersen CT, Sorich MJ et al. (2011) Low relative abundances of the mucolytic bacterium *Akkermansia muciniphila* and *Bifidobacterium spp.* in feces of children with autism. *Applied and Environmental Microbiology* 77: 6718–6721.
22. Murphy EF, Cotter PD, Hogan A et al. (2013) Divergent metabolic outcomes arising from targeted manipulation of the gut microbiota in diet-induced obesity. *Gut* 62: 220–226.

23. Bendtsen KM, Hansen CHF, Krych L et al. (2017) Immunological effects of reduced mucosal integrity in the early life of BALB/c mice. *PLoS ONE* 12: e0176662.

24. Hansen AK (2014) Mechanisms behind bacterial impact on animal models. In: Hansen AK and Nielsen DS (eds) *Handbook of Laboratory Animal Bacteriology*, 2nd edn. Boca Raton, FL: CRC Press, pp. 103–126.

25. Bendtsen KM, Hansen CHF, Krych L et al. (2017) Effect of early-life gut mucosal compromise on disease progression in NOD mice. *Comparative Medicine* 67: 388–399.

26. Bendtsen KM, Tougaard P and Hansen AK (2018) An early life mucosal insult temporarily decreases acute oxazolone-induced inflammation in mice. *Inflammation* 41: 1437–1447.

27. Klein L, Kyewski B, Allen PM et al. (2014) Positive and negative selection of the T cell repertoire: What thymocytes see (and don't see). *Nature Reviews Immunology* 14: 377–391.

28. Itoh M, Takahashi T, Sakaguchi N et al. (1999) Thymus and autoimmunity: Production of CD25+CD4+ naturally anergic and suppressive T cells as a key function of the thymus in maintaining immunologic self-tolerance. *Journal of Immunology* 162: 5317–5326.

29. Firan M, Dhillon S, Estess P et al. (2006) Suppressor activity and potency among regulatory T cells is discriminated by functionally active CD44. *Blood* 107: 619–627.

30. Jordan MS, Boesteanu A, Reed AJ et al. (2001) Thymic selection of CD4+CD25+ regulatory T cells induced by an agonist self-peptide. *Nature Immunology* 2: 301–306.

31. Apostolou I and von Boehmer H (2004) In vivo instruction of suppressor commitment in naive T cells. *Journal of Experimental Medicine* 199: 1401–1408.

32. Chen WJ, Jin WW, Hardegen N et al. (2003) Conversion of peripheral CD4+CD25- naive T cells to CD4+CD25+ regulatory T cells by TGF-beta induction of transcription factor Foxp3. *Journal of Experimental Medicine* 198: 1875–1886.

33. Kretschmer K, Apostolou I, Hawiger D et al. (2005) Inducing and expanding regulatory T cell populations by foreign antigen. *Nature Immunology* 6: 1219–1227.

34. Worbs T, Bode U, Yan S et al. (2006) Oral tolerance originates in the intestinal immune system and relies on antigen carriage by dendritic cells. *Journal of Experimental Medicine* 203: 519–527.

35. Hadis U, Wahl B, Schulz O et al. (2011) Intestinal tolerance requires gut homing and expansion of FoxP3+ regulatory T cells in the lamina propria. *Immunity* 34: 237–246.

36. Haribhai D, Williams JB, Jia S et al. (2011) A requisite role for induced regulatory T cells in tolerance based on expanding antigen receptor diversity. *Immunity* 35: 109–122.

37. Huang YJ, Haist V, Baumgartner W et al. (2014) Induced and thymus-derived Foxp3+ regulatory T cells share a common niche. *European Journal of Immunology* 44: 460–468.

38. Ni J, Chen SF and Hollander D (1996) Effects of dextran sulphate sodium on intestinal epithelial cells and intestinal lymphocytes. *Gut* 39: 234–241.

39. Fredin MF, Elgbratt K, Svensson D et al. (2007) Dextran sulfate sodium-induced colitis generates a transient thymic involution—Impact on thymocyte subsets. *Scandinavian Journal of Immunology* 65: 421–429.

40. Sasaki S, Ishida Y, Nishio N et al. (2008) Thymic involution correlates with severe ulcerative colitis induced by oral administration of dextran sulphate sodium in C57BL/6 mice but not in BALB/c mice. *Inflammation* 31: 319–328.

41. Trottier MD, Irwin R, Li Y et al. (2012) Enhanced production of early lineages of monocytic and granulocytic cells in mice with colitis. *Proceedings of the National Academy of Sciences of the United States of America* 109: 16594–16599.

42. Clarke AG and Kendall MD (1994) The thymus in pregnancy: The interplay of neural, endocrine and immune influences. *Immunology Today* 15: 545–551.

43. Fauci AS (1976) Mechanisms of corticosteroid action on lymphocyte subpopulations. II. Differential effects of in vivo hydrocortisone, prednisone and dexamethasone on in vitro expression of lymphocyte function. *Clinical and Experimental Immunology* 24: 54–62.

44. Wang SD, Huang KJ, Lin YS et al. (1994) Sepsis-induced apoptosis of the thymocytes in mice. *Journal of Immunology* 152: 5014–5021.

45. Teshima H, Sogawa H, Kihara H et al. (1991) Influence of stress on the maturity of T-cells. *Life Sciences* 49: 1571–1581.

46. Melgar S, Karlsson A and Michaelsson EM (2005) Acute colitis induced by dextran sulfate sodium progresses to chronicity in C57BL/6 but not in BALB/c mice: Correlation between symptoms and inflammation. *American Journal of Physiology: Gastrointestinal and Liver Physiology* 288: G1328–G1338.

47. Cooper HS, Murthy SNS, Shah RS et al. (1993) Clinicopathologic study of dextran sulfate sodium experimental murine colitis. *Laboratory Investigation* 69: 238–249.

48. Murthy SNS, Cooper HS, Shim H et al. (1993) Treatment of dextran sulfate sodium-induced murine colitis by intracolonic cyclosporin. *Digestive Diseases and Sciences* 38: 1722–1734.

49. Dieleman LA, Ridwan BU, Tennyson GS et al. (1994) Dextran sulfate sodium-induced colitis occurs in severe combined immunodeficient mice. *Gastroenterology* 107: 1643–1652.

50. De Filippo K, Henderson RB, Laschinger M et al. (2008) Neutrophil chemokines KC and

macrophage-inflammatory protein-2 are newly synthesized by tissue macrophages using distinct TLR signaling pathways. *Journal of Immunology* 180: 4308–4315.

51. Denning TL, Wang YC, Patel SR et al. (2007) Lamina propria macrophages and dendritic cells differentially induce regulatory and interleukin 17-producing T cell responses. *Nature Immunology* 8: 1086–1094.

52. Berlin C, Berg EL, Briskin MJ et al. (1993) Alpha 4 beta 7 integrin mediates lymphocyte binding to the mucosal vascular address in MADCAM-1. *Cell* 74: 185–195.

53. Cepek KL, Shaw SK, Parker CM et al. (1994) Adhesion between epithelial cells and T lymphocytes mediated by E-cadherin and the alpha E beta 7 integrin. *Nature* 372: 190–193.

54. Karecla PI, Bowden SJ, Green SJ et al. (1995) Recognition of E-cadherin on epithelial cells by the mucosal T cell integrin alpha M290 beta 7 (alpha E beta 7). *European Journal of Immunology* 25: 852–856.

55. Wagner N, Lohler J, Kunkel EJ et al. (1996) Critical role for beta7 integrins in formation of the gut-associated lymphoid tissue. *Nature* 382: 366–370.

56. Itoi H, Fujimori Y, Tsutsui H et al. (2004) Differential upregulation of interleukin-18 receptor alpha chain between CD4+ and CD8+ T cells during acute graft-versus-host disease in mice. *Journal of Interferon and Cytokine Research* 24: 291–296.

57. Raué HP, Brien JD, Hammarlund E et al. (2004) Activation of virus-specific CD8+ T cells by lipopolysaccharide-induced IL-12 and IL-18. *Journal of Immunology* 173: 6873–6881.

58. Yoshimoto T, Takeda K, Tanaka T et al. (1998) IL-12 up-regulates IL-18 receptor expression on T cells, Th1 cells, and B cells: Synergism with IL-18 for IFN-gamma production. *Journal of Immunology* 161: 3400–3407.

59. Dieleman LA, Elson CO, Tennyson GS et al. (1996) Kinetics of cytokine expression during healing of acute colitis in mice. *American Journal of Physiology: Gastrointestinal and Liver Physiology* 271: G130–G136.

60. Guimbaud R, Bertrand V, Chauvelot-Moachon L et al. (1998) Network of inflammatory cytokines and correlation with disease activity in ulcerative colitis. *American Journal of Gastroenterology* 93: 2397–2404.

61. Arai Y, Takanashi H, Kitagawa H et al. (1998) Involvement of interleukin-1 in the development of ulcerative colitis induced by dextran sulfate sodium in mice. *Cytokine* 10: 890–896.

62. Elgbratt K, Bjursten M, Willen R et al. (2007) Aberrant T-cell ontogeny and defective thymocyte and colonic T-cell chemotactic migration in colitis-prone Galphai2-deficient mice. *Immunology* 122: 199–209.

63. Da Silva APB, Pollett A, Rittling SR et al. (2006) Exacerbated tissue destruction in DSS-induced acute colitis of OPN-null mice is associated with downregulation of TNF-alpha expression and non-programmed cell death. *Journal of Cellular Physiology* 208: 629–639.

64. Elgbratt K, Kurlberg G, Hahn-Zohric M et al. (2010) Rapid migration of thymic emigrants to the colonic mucosa in ulcerative colitis patients. *Clinical and Experimental Immunology* 162: 325–336.

65. Franco MA and Greenberg HB (1999) Immunity to rotavirus infection in mice. *Journal of Infectious Diseases* 179: S466–S469.

66. Muller KM, Luedecker CJ, Udey MC et al. (1997) Involvement of e-cadherin in thymus organogenesis and thymocyte maturation. *Immunity* 6: 257–264.

67. Kutlesa S, Wessels JT, Speiser A et al. (2002) E-cadherin-mediated interactions of thymic epithelial cells with CD103+ thymocytes lead to enhanced thymocyte cell proliferation. *Journal of Cell Science* 115: 4505–4515.

68. Beura LK, Hamilton SE, Bi K et al. (2016) Normalizing the environment recapitulates adult human immune traits in laboratory mice. *Nature* 532: 512–516.

69. Peaudecerf L, dos Santos PR, Boudil A et al. (2011) The role of the gut as a primary lymphoid organ: CD8αα intraepithelial T lymphocytes in euthymic mice derive from very immature CD44+ thymocyte precursors. *Mucosal Immunology* 4: 93–101.

70. Rodriguez-Galan MC, Bream JH, Farr A et al. (2005) Synergistic effect of IL-2, IL-12, and IL-18 on thymocyte apoptosis and Th1/Th2 cytokine expression. *Journal of Immunology* 174: 2796–2804.

71. Schwab C, Berry D, Rauch I et al. (2014) Longitudinal study of murine microbiota activity and interactions with the host during acute inflammation and recovery. *ISME Journal* 8: 1101–1114.

72. De Fazio L, Cavazza E, Spisni E et al. (2014) Longitudinal analysis of inflammation and microbiota dynamics in a model of mild chronic dextran sulfate sodium-induced colitis in mice. *World Journal of Gastroenterology* 20: 2051–2061.

73. Jamieson AM, Diefenbach A, McMahon CW et al. (2002) The role of the NKG2D immunoreceptor in immune cell activation and natural killing. *Immunity* 17: 19–29.

74. Kunikata T, Torigoe K, Ushio S et al. (1998) Constitutive and induced IL-18 receptor expression by various peripheral blood cell subsets as determined by anti-hIL-18R monoclonal antibody. *Cellular Immunology* 189: 135–143.

75. Budd RC, Cerottini JC, Horvath C et al. (1987) Distinction of virgin and memory T lymphocytes. Stable acquisition of the Pgp-1 glycoprotein concomitant with antigenic stimulation. *Journal of Immunology* 138: 3120–3129.

76. Nakahira M, Tomura M, Iwasaki M et al. (2001) An absolute requirement for STAT4 and a role for

IFN-gamma as an amplifying factor in IL-12 induction of the functional IL-18 receptor complex. *Journal of Immunology* 167: 1306–1312.

77. Holmkvist P, Roepstorff K, Uronen-Hansson H et al. (2015) A major population of mucosal memory CD4^{+} T cells, coexpressing IL-18Rα and DR3, display innate lymphocyte functionality. *Mucosal Immunology* 8: 545–558.

78. Coder BD, Wang HJ, Ruan LH et al. (2015) Thymic involution perturbs negative selection leading to autoreactive T cells that induce chronic inflammation. *Journal of Immunology* 194: 5825–5837.